HAL open science

Electrochemical advanced oxidation processes using novel electrode materials for mineralization and biodegradability enhancement of nanofiltration concentrate of landfill leachates

Marwa El Kateb, Clément Trellu, Alaa Darwich, Matthieu Rivallin, Mikhael Bechelany, Sakthivel Nagarajan, Stella Lacour, Nizar Bellakhal, Geoffroy Lesage, Marc Heran, et al.

To cite this version:

Marwa El Kateb, Clément Trellu, Alaa Darwich, Matthieu Rivallin, Mikhael Bechelany, et al.. Electrochemical advanced oxidation processes using novel electrode materials for mineralization and biodegradability enhancement of nanofiltration concentrate of landfill leachates. Water Research, 2019, 162, pp.446-455. 10.1016/j.watres.2019.07.005 . hal-02278696

HAL Id: hal-02278696

https://hal.umontpellier.fr/hal-02278696v1

Submitted on 25 Oct 2021

HAL is a multi-disciplinary open access archive for the deposit and dissemination of scientific research documents, whether they are published or not. The documents may come from teaching and research institutions in France or abroad, or from public or private research centers.

L'archive ouverte pluridisciplinaire **HAL**, est destinée au dépôt et à la diffusion de documents scientifiques de niveau recherche, publiés ou non, émanant des établissements d'enseignement et de recherche français ou étrangers, des laboratoires publics ou privés.

Distributed under a Creative Commons Attribution - NonCommercial 4.0 International License

Version of Record: https://www.sciencedirect.com/science/article/pii/S0043135419306049
Manuscript_04ede0bf20a6159a01cfcef343ebc6a4

Electrochemical advanced oxidation processes using novel electrode materials for mineralization and biodegradability enhancement of nanofiltration concentrate of landfill leachates.

Marwa El Kateb[1,2,4], Clément Trellu[1,3,*], Alaa Darwich[1], Matthieu Rivallin[1], Mikhael Bechelany[1], Sakthivel Nagarajan[1], Stella Lacour[1], Nizar Bellakhal[4], Geoffroy Lesage[1], Marc Héran[1], Marc Cretin[1,*]

[1] IEM, Univ Montpellier, CNRS, ENSCM, Montpellier, France

[2] Université de Tunis El Manar, Faculté des Sciences de Tunis, 2092 Tunis, Tunisie

[3] Laboratoire Géomatériaux et Environnement, LGE – Université Paris-Est, EA 4508, UPEM, 77454 Marne-la-Vallée, France

[4] Université de Carthage, Institut National des Sciences Appliquées et de Technologie, Laboratoire d'Echo-Chimie, 1080 Tunis, Tunisie

Manuscript submitted to Water Research for consideration

* Corresponding Author:

clement.trellu@u-pem.fr

+33 1 49 32 90 42

© 2019 published by Elsevier. This manuscript is made available under the CC BY NC user license
https://creativecommons.org/licenses/by-nc/4.0/

Graphical abstract

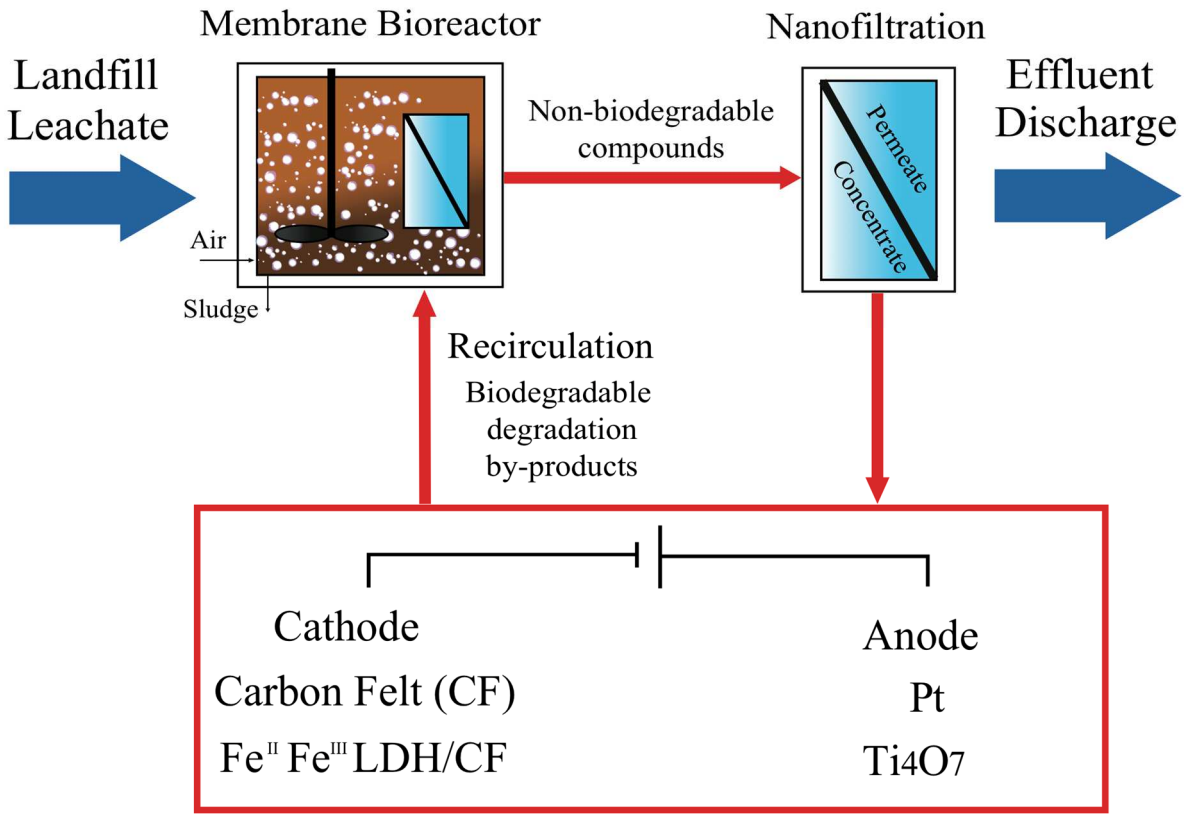

Electrochemical Advanced Oxidation Processes
Homogeneous/Heterogeneous electro-Fenton
Anodic Oxidation

Abstract

The objective of this study was to implement electrochemical advanced oxidation processes (EAOPs) for mineralization and biodegradability enhancement of nanofiltration (NF) concentrate from landfill leachate initially pre-treated in a membrane bioreactor (MBR). Raw carbon felt (CF) or $Fe^{II}Fe^{III}$ layered double hydroxides-modified CF were used for comparing the efficiency of homogeneous and heterogeneous electro-Fenton (EF), respectively. The highest mineralization rate was obtained by heterogeneous EF: 96% removal of dissolved organic carbon (DOC) was achieved after 8 h of electrolysis at circumneutral initial pH (pH_0 = 7.9) and at 8.3 mA cm^{-2}. However, the most efficient treatment strategy appeared to be heterogeneous EF at 4.2 mA cm^{-2} combined with anodic oxidation using Ti_4O_7 anode (energy consumption = 0.11 kWh g^{-1} of DOC removed). Respirometric analyses under similar conditions than in the real MBR emphasized the possibility to recirculate the NF retentate towards the MBR after partial mineralization by EAOPs in order to remove the residual biodegradable by-products and improve the global cost effectiveness of the process. Further analyses were also performed in order to better understand the fate of organic and inorganic species during the treatment, including acute toxicity tests (Microtox®), characterization of dissolved organic matter by three-dimensional fluorescence spectroscopy, evolution of inorganic ions (ClO_3^-, NH_4^+ and NO_3^-) and identification/quantification of degradation by-products such as carboxylic acids. The obtained results emphasized the interdependence between the MBR process and EAOPs in a combined treatment strategy. Improving the retention in the MBR of colloidal proteins would improve the effectiveness of EAOPs because such compounds were identified as the most refractory. Enhanced nitrification would be also required in the MBR because of the release of NH_4^+ from mineralization of refractory organic nitrogen during EAOPs.

Keywords

Electro-Fenton; Anodic oxidation; Modified carbon felt; Sub-stoichiometric titanium oxide; Landfill leachate; Biodegradability.

1. Introduction

Rainwater percolation through waste layers of landfills generates leachates containing a complex mixture of dissolved organic matter (DOM), inorganic compounds, heavy metals, and xenobiotic organic substances (Kjeldsen et al., 2002), which represents a significant hazard for the environment.

The implementation of a membrane bioreactor (MBR) followed by a nanofiltration (NF) step is one of the most efficient treatment strategy currently used for management of landfill leachates (Campagna et al., 2013; Amaral et al., 2016). However, NF is only a separation process. Biorefractory organic pollutants are accumulated and concentrated. Thus, the concentrate becomes an important residual issue for this treatment strategy (Van der Bruggen et al., 2003; Zhang et al., 2009, 2013). Landfill discharge of the concentrate is commonly performed. However, some national regulations do not allow such practice and it clearly does not fix the long-term issue. In recent years, several processes have been investigated and applied at industrial scale for the treatment of NF concentrate. For example, adsorption processes are effective to remove organic matters in NF concentrate, but they are strongly limited by the high organic charge of such effluents compared to the adsorption capacity of adsorbent materials. Besides, membrane distillation and evaporation processes are substantially limited by the high cost of equipment and energy consumption (Cui et al., 2018).

During the last two decades, electrochemical advanced oxidation processes (EAOPs) have received great attention for efficient degradation of a large range of hazardous and biorefractory organic compounds. They are based on *in situ* electrogeneration of hydroxyl radicals ($^{\bullet}OH$), a non-selective and powerful oxidizing agent ($E^{\circ}(^{\bullet}OH/H_2O) = 2.80$ V *vs* SHE) (Brillas et al., 2009; Comninellis et al., 2008; Martínez-Huitle et al., 2015; Panizza and Cerisola, 2009). EAOPs provide also several technical advantages such as high versatility,

easy operation, possibility for automation and low consumption of chemical reagents (Radjenovic and Sedlak, 2015; Sirés et al., 2014). However, complete mineralization of organic compounds requires high energy consumption. Therefore, the combination of EAOPs with biological processes is currently more and more investigated as a feasible option for improving the global cost-effectiveness of the process (Oller et al., 2011; Ganzenko et al., 2014, 2018; Trellu et al., 2016a; Olvera-Vargas et al., 2015). In order to achieve reliable conclusions, the accurate assessment of biodegradability enhancement by EAOPs requires the use of proper measurement tools such as respirometric methods (Reuschenbach et al., 2003).

Anodic oxidation (AO) and electro-Fenton (EF) are the most popularized EAOPs (Brillas et al., 2009; Panizza and Cerisola, 2009; Martínez-Huitle et al., 2015; Oturan et al., 2015). AO is based on the generation of hydroxyl radicals ($^{\bullet}OH$) via water oxidation at the surface of anodes (M) with high overvoltage for oxygen evolution reaction (Eq. 1) (Panizza and Cerisola, 2009; Trellu et al., 2017; Özcan et al., 2008), while $^{\bullet}OH$ are generated homogeneously in the bulk during the EF process through the Fenton's reaction (Eq. 2) (Brillas et al., 2009; Ma et al., 2016; Zhang et al., 2007). H_2O_2 and iron (II) are continuously electrogenerated at the cathode by reduction of dissolved oxygen (Eq. 3) and iron (III) reduction (Eq. 4), respectively. External oxygen supply is required and an iron source must be either initially added at catalytic amount to the treated solution (homogeneous EF) or embedded onto suitable electrode materials (heterogeneous EF).

$$M + H_2O \longrightarrow M(^{\bullet}OH) + H^+ + e^- \qquad \text{(Eq. 1)}$$

$$Fe^{2+} + H_2O_2 + H^+ \longrightarrow Fe^{3+} + {}^{\bullet}OH + H_2O \qquad \text{(Eq. 2)}$$

$$O_{2(g)} + 2H^+ + 2e^- \longrightarrow H_2O_2 \qquad \text{(Eq. 3)}$$

$$Fe^{3+} + e^- \longrightarrow Fe^{2+} \qquad \text{(Eq. 4)}$$

Homogeneous EF requires external iron source and acidic pH (*i.e.* pH 2.5 – 3.5) that prevents iron precipitation (Brillas et al., 2009). Besides, heterogeneous EF using for example pyrite (Ammar et al., 2015) or iron loaded sepiolite (Iglesias et al., 2013) as iron source has been developed in order to operate the process over a wide pH range (Ganiyu et al., 2018; Poza-Nogueiras et al., 2018). Innovative electrodes have been also synthesized and studied as both heterogeneous catalyst source and cathode materials (Zhang et al., 2012; Wang et al., 2013; García-Rodríguez et al., 2016; Ganiyu et al., 2017a). Particularly, the modification of raw carbon felt (CF) with CoFe or $Fe^{II}Fe^{III}$-layered double hydroxide (LDH) also led to an increase of the electroactive surface area, which in turn improved the generation of H_2O_2 and the global efficiency of the heterogeneous EF process (Ganiyu et al., 2017a, 2018). However, to the best of our knowledge, none study focused on the application of such promising electrodes for the treatment of real wastewaters.

As regards to anode materials, sub-stoichiometric titanium oxides (especially Ti_4O_7) recently received great attention for application in wastewater treatment by AO (Guo et al., 2016; Ganiyu et al., 2016; Trellu et al., 2018b). Ti_4O_7 anode is able to generate large amounts of physisorbed hydroxyl radicals ($Ti_4O_7(^{\bullet}OH)$) for the degradation and mineralization of organic contaminants. Besides, this material has the potential to become a low-cost anode compared to the well known boron-doped diamond anode (Ganiyu et al., 2017b; Trellu et al., 2018b). However, to the best of our knowledge, such anode material has also still not been applied for the treatment of real effluents.

The objective of this study was to investigate the application of these novel electrode materials for the treatment of a NF concentrate of landfill leachate initially pre-treated in a MBR, which represents an important challenge for environmental engineering. Various configurations (*i.e.* homogeneous EF, heterogeneous EF, heterogeneous EF/AO) and operating conditions were studied. The efficiency for mineralization of organic compounds

was compared. A particular attention was also given to the understanding of mineralization mechanisms by using various analytical tools: (i) DOM was characterized by three-dimensional excitation and emission matrix fluorescence (3DEEM), (ii) degradation by-products such as short-chain carboxylic acids were identified and quantified by ion-exclusion HPLC, and (iii) inorganic ions released during the mineralization process were identified and quantified by ion chromatography. Moreover, acute toxicity of the effluent was assessed by Microtox® analysis and the possibility to use such EAOPs as a pre-treatment before recirculation towards the MBR was assessed by using respirometric method under similar conditions than in the real industrial MBR. Finally, recommendations were given by taking into consideration the interdependence of MBR process and EAOP in a combined treatment strategy.

2. Materials and methods

2.1 Chemicals

For the preparation of $Fe^{II}Fe^{III}$-LDH modified CF, iron III nitrate nonahydrate $Fe(NO_3)_3.9H_2O$ (CAS 7782-61-8, 98% purity), iron II sulfate heptahydrate $FeSO_4.7H_2O$ (CAS 7782-63-0, >99% purity), urea $CO(NH_2)_2$ (CAS 57-13-6) and ammonium fluoride NH_4F (CAS 12125-01-8, 99% purity) were supplied by Sigma Aldrich. Ultra-pure water (Millipore Mill-Q system, resistivity >18 MΩ.cm at 25 °C) was used for the preparation of all solutions.

2.2 Landfill leachate (NF concentrate)

The NF concentrate was collected from a landfill leachate wastewater treatment plant (WWTP) in the south of France. The raw landfill leachate was initially treated in a MBR, then

123 followed by a NF step. The concentrate from the NF step was collected and stored in a
124 refrigerator at 4 °C.

125

126 **2.3 Electrochemical setup and electrode materials**

127 Experiments were conducted in an undivided cylindrical glass containing 220 mL of NF
128 concentrate at room temperature (25 °C). The electrochemical cell was similar to the one used
129 in several previous studies (Ganiyu et al., 2016; Trellu et al., 2016b). Either raw CF (for
130 homogeneous EF) or $Fe^{II}Fe^{III}$-LDH modified CF (for heterogeneous EF) was employed as
131 cathode (20 x 6 cm; 120 cm^2), positioned on the inner wall of the cylindrical cell. CF (99.0%,
132 6.35 mm thick) was provided by Alfa Aesar. $Fe^{II}Fe^{III}$-LDH modified CF was prepared by *in-*
133 *situ* solvothermal process as reported elsewhere (Ganiyu et al., 2018). LDH coating was 0.62
134 ± 0.04 mg cm^{-2}, which was also in agreement with what has been reported previously (Ganiyu
135 et al., 2018). For homogeneous EF experiments, 0.2 mM of Fe^{2+} was added to the solution
136 and initial pH was adjusted at 3 (values usually reported as optimal). For heterogeneous EF
137 experiments, none Fe^{2+} was externally added and pH was not initally adjusted.
138 The anode was either a 24 cm^2 (3 x 8 cm) platinum mesh (for homogeneous and
139 heterogeneous EF) or a 32 cm^2 (4 x 8 cm) Ti_4O_7 thin film plasma deposited on Ti substrate
140 (for heterogeneous EF/AO) from Saint-Gobain Research Provence, France. Ti_4O_7 powder
141 used for plasma deposition was prepared by carbothermal reduction of TiO_2 as already
142 reported by our group (Ganiyu et al., 2016, 2017b). These rectuganlar-shaped anodes were
143 placed at the center of the cylindrical electrochemical cell, with an average interelectrode
144 distance of 3 cm.
145 Electrodes were connected to a DC power supply (CNB Electronique) with applied current set
146 at 1000 mA (j = 8.3 mA cm^{-2}, calcultated from the cathode surface, which is the working

electrode during the EF process) or 500 mA (j = 4.2 mA cm^{-2}). A magnetic stirrer was used to improve mass transport of chemical species toward/from the electrodes. The solution was saturated with O_2 by bubbling compressed air through a glass frit 10 min before starting the experiments and all along the electrolysis. The conductivity of the NF concentrate was high enough to ensure the electrolysis without any additional supporting electrolyte. For comparison, a reference experiment was also carried out using raw carbon felt cathode, Pt anode, without adding any source of iron and without initial pH adjustment.

2.4 Dissolved organic carbon and chemical oxygen demand analysis

Mineralization rate of NF concentrate was determined by total organic carbon (TOC) analyses using the Shimadzu TOC-L analyzer based on the 680 °C combustion catalytic oxidation method. All samples were filtrated through 0.45 µm regenerated cellulose (RC) membrane filters. Therefore, results are reported as dissolved organic carbon (DOC).

Chemical oxygen demand (COD) was analyzed by the method AFNOR NFT 90-101 using Hach COD kits.

2.5 Respirometric method for the determination of biodegradability

Biodegradability was assessed with a BM-T Advance Respirometer (SURCIS S.L, Spain), which consists in a 1 L capacity vessel, provided with an oxygen probe (Hamilton) and temperature control system. The activated sludge used in the bioassays was collected from the aerated tank of the landfill leachate WWTP using MBR and was thus acclimatized to the effluent. The samples were evaluated without pH adjustment because of the high buffer capacity of the landfill leachate samples. Continuous aeration and agitation were applied to

170 ensure air saturation conditions. Temperature was maintained at 20 °C during the tests and the
171 standardization with sodium acetate method was applied (conversion rate adjustment
172 according to instructions given by the respirometer's manufacturer). In order to inhibit the
173 nitrification process and measure the sample effect only on the heterotrophic bacteria, 1.5 mg
174 $gVSS^{-1}$ of N-allylthiourea was added before the beginning of each trial.

175 For biodegradability assays, 700 mL of endogenous activated sludge and 300 mL of target
176 sample were introduced in the respirometer. The biodegradability of samples pre-treated by
177 EAOPs was assessed through R tests (Fig. SI 1). The ratio between biodegradable COD
178 (bCOD) and DOC (bCOD/DOC) was used for determination of the biodegradable character
179 of each sample. A biodegradability enhancement index (BE) was calculated by using Eq. 5.

180 $$BE = \frac{\left(\frac{bCOD_t}{DOC_t}\right)}{\left(\frac{bCOD_0}{DOC_0}\right)} \qquad \text{(Eq. 5)}$$

181 Where $bCOD_t$ and DOC_t are bCOD (in $gO_2\ L^{-1}$) and DOC (in $gC\ L^{-1}$) after t hours of
182 treatment by EAOPs.

183

184 **2.6 Characterization of dissolved organic matter by three-dimensional excitation and**
185 **emission matrix fluorescence (3DEEM)**

186 Natural organic matter was characterized by 3DEEM fluorescence using a Perkin-Elmer LS-
187 55 spectrometer (USA). The dilution factor was 200 for all samples. The procedure reported
188 by Jacquin et al. (2017) was used for fluorescence spectra acquisition and data extraction.
189 Chen et al. (2003) divided fluorescence spectra into five different areas corresponding to
190 different groups of fluorophores, *i.e.* regions I and II for aromatic proteins, region III for
191 fulvic acid-like (FA-like) fluorophores, region IV for soluble microbial by-product-like
192 (SMP-like) fluorophores and region V for humic acid-like (HA-like) fluorophores (Chen et

193 al., 2003). Similarly to the study of Jacquin et al. (2017), 3DEEM results were analyzed by
194 taking into consideration only 3 different zones, *i.e.* zone I' for region I + II (aromatic
195 proteins), zone II' for region IV (SMP-like) and zone III' for region III + V (HA + FA-like).
196 Calculation of the volume of fluorescence in these different zones was achieved following the
197 method from Jacquin et al. (2017).

198

199 The procedures for ICP-MS analysis, toxicity test (Microtox®), identification/quantification of
200 inorganic ions and identification/quantification of short-chain carboxylic acids are provided in
201 Supplementary Information (SI)

202

203 3. Results and Discussion

204 3.1 Characterization of the NF concentrate effluent

205 The characteristics of the NF concentrate are presented in SI (Table SI 1). The effluent was a
206 dark brown liquid having a slightly alkaline pH and high organic charge. The conductivity
207 (3.1 mS cm^{-1}) was between 3 and 10 times lower than values reported in the literature (10 –
208 33 $mS.cm^{-1}$) (Li et al., 2015; Hu et al., 2018; Xu et al., 2017). This might be ascribed to the
209 high diversity of landfill leachate and to a lower retention of ionic species by the NF step. In
210 fact, the concentration factor of divalent (Mg^{2+} and Ca^{2+}) and monovalent (Na^{+} and K^{+})
211 inorganic cations was only 3.1 ± 0.3 and 1.7 ± 0.2, respectively. Monovalent ions are less
212 retained by the NF membrane because of lower charge interactions (Van der Bruggen et al.,
213 2004). The COD content (2.1 gO_2 L^{-1}) of the NF concentrate was also in the low range of
214 values usually reported in the literature (1.7 – 5.5 gO_2 L^{-1}) (Li et al., 2015; Hu et al., 2018; Xu

215 et al., 2017) because of (i) operation of the NF process with a lower concentration factor
216 and/or (ii) lower initial organic loading rate of the effluent pre-treated by the MBR.

217 The ratio between bCOD and total COD or total DOC was low (bCOD/COD = 0.12 or
218 bCOD/DOC = 0.26), thus indicating the low biodegradability of the concentrate owing to the
219 presence of high-molecular weight and non-biodegradable compounds. A high concentration
220 of nitrate ([NO_3^-] = 90 mg L^{-1}) was observed due to the complete nitrification of NH_4^+ in the
221 MBR and a partial denitrification in the anoxic tank. As regards to metals, Sr ion was the
222 most concentrated (6.0 mg L^{-1}) and high concentrations of As (0.38 mg L^{-1}) and Cr (0.67 mg
223 L^{-1}) ions were also reported. These metals are released by different wastes discarded in
224 landfills such as glass products (Ponthieu et al., 2007), fluorescent lights and ceramics
225 (Mahindrakar and Rathod, 2018). Besides, the high concentration of Sb (1.2 mg L^{-1}) indicates
226 an important contamination from plastic decomposition (Westerhoff et al., 2008).

227

228 **3.2 Mineralization efficiency by EAOPs**

229 Various experiments were performed in order to evaluate the efficiency of different EAOPs
230 (*i.e.* homogeneous EF, heterogeneous EF, heterogeneous EF/AO).

231 First, volatilization and adsorption phenomena were evidenced by bubbling oxygen into the
232 electrochemical reactor without any current applied. Under these conditions, DOC content
233 decreased and reached a plateau after 1 h with around 16±2% removal due to volatilization of
234 volatile organic compounds and adsorption of hydrophobic compounds on CF. Besides, it was
235 also observed that initial pH adjustment at 3 decreased the DOC value by 15±5% because of
236 the precipitation of humic acids.

237 Second, experiments were carried out under constant current density applied to the electrodes.
238 As shown in Fig. 1A, 96% of DOC removal was obtained after 8 h of electrolysis by

239 heterogeneous EF with an applied current density of 8.3 mA cm^{-2}. The excellent
240 mineralization efficiency achieved without any initial pH adjustment was ascribed to
241 heterogeneous EF reaction occurring on the surface of the $Fe^{II}Fe^{III}$-LDH catalyst, which
242 catalyzed the decomposition of H_2O_2 to generate large amounts of hydroxyl radicals $^{\bullet}OH$
243 (Ganiyu et al., 2018). By comparison, only 59% removal of DOC was obtained in the
244 reference experiment with analogous operating conditions but using raw CF as cathode
245 instead of $Fe^{II}Fe^{III}$-LDH modified CF, thus highlighting the benefits obtained from the use of
246 the modified cathode. Heterogeneous EF was also even more efficient than conventional
247 homogeneous EF (90% removal of DOC after 8 h) with external addition of iron catalyst (0.2
248 mmol L^{-1}) and initial adjustment of pH at 3. Therefore, $Fe^{II}Fe^{III}$-LDH modified CF appeared
249 as an ideal cathode material that enhances the mineralization efficiency of the EF process and
250 avoids both initial pH adjustment and external addition of iron. The stability and reusability of
251 the prepared $Fe^{II}Fe^{III}$-LDH modified CF cathode was assessed by reusing the same electrode
252 for 4 successive electrolysis cycles (Fig. 2). The slight but continuous decrease of the
253 efficiency could be ascribed to (i) the initial loss of loosely bounded $Fe^{II}Fe^{III}$-LDH at the
254 external surface of the CF substrate due to vigorous stirring and/or (ii) iron leaching at acidic
255 pH for which $Fe^{II}Fe^{III}$-LDH coating is less stable. Indeed, a progressive reduction of pH to
256 values in the range 3 - 4 was noticed during electrolysis, which was explained by the
257 generation of short-chain carboxylic acids. This leaching phenomenon was confirmed by
258 comparison of SEM images of raw CF, $Fe^{II}Fe^{III}$-LDH modified CF before use and $Fe^{II}Fe^{III}$-
259 LDH modified CF after 4 cycles of electrolysis (Fig. SI 2). While an extensive growth on the
260 CF of dense platelets of $Fe^{II}Fe^{III}$-LDH with uneven and porous structure was initially
261 obtained, a partial degradation of the global $Fe^{II}Fe^{III}$-LDH structure was observed after 4
262 cycles. Thus, in order to avoid the depletion of the catalyst, a continuous pH control

263 regulation would be recommended rather than a unique pH re-adjustment at the end of the
264 treatment.

265 Third, experiments were also performed at lower current density (4.2 mA cm^{-2}, Fig. 1B).
266 Lower DOC removal rates were obtained, e.g. 72% *vs* 96% removal of DOC after 8 h of
267 treatment by heterogeneous EF at 4.2 mA cm^{-2} and 8.3 mA cm^{-2}, respectively. Indeed, high
268 current density enhances the generation of hydrogen peroxide and regeneration rate of Fe(II).
269 Thus, further $^{\bullet}OH$ are produced for oxidation and mineralization of organic compounds.

270 Fourth, the influence of the anode material was also investigated (Fig. 1B). After 8h of
271 treatment by heterogeneous EF/AO using Ti_4O_7 anode at 4.2 mA cm^{-2}, 77% removal of DOC
272 was achieved, compared to 72% by heterogeneous EF using Pt anode. The higher efficiency
273 of Ti_4O_7 anode was ascribed to the generation at the anode surface of physisorbed $Ti_4O_7(^{\bullet}OH)$
274 with great oxidation ability, because of the higher overvoltage for oxygen evolution reaction
275 (>0.7 V), compared to Pt anode (<0.4 V) (Trellu et al., 2018a; Ganiyu et al., 2018). Therefore,
276 by taking also into consideration the lower cost of Ti_4O_7, this anode material appeared as a
277 suitable electrode to combine AO and EF processes.

278

279

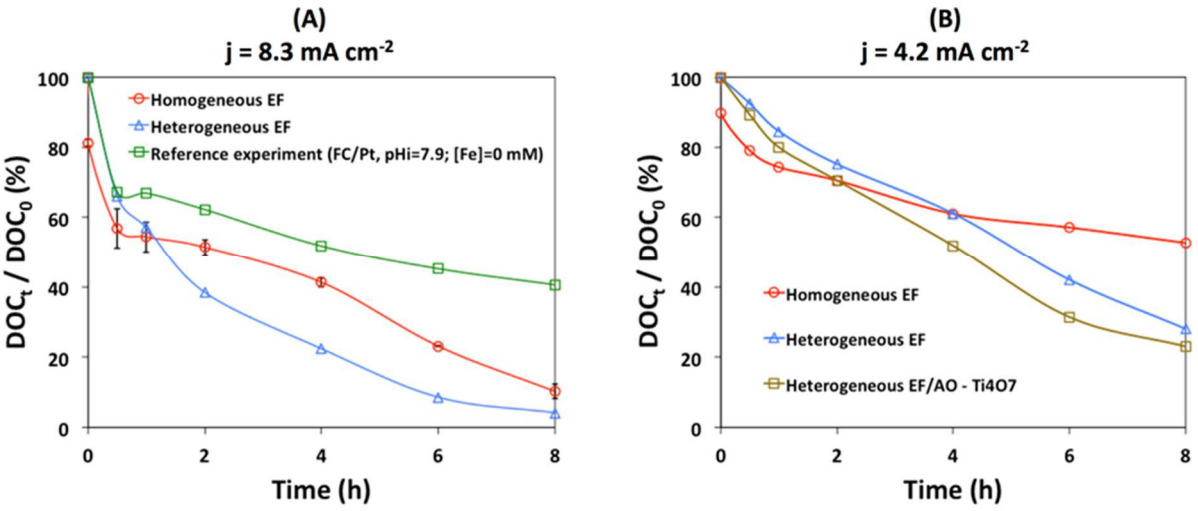

Figure 1 – DOC removal efficiency *vs* time during the mineralization of NF concentrate. Comparison of different configurations and operating conditions.

(A) j = 8.3 mA cm^{-2} : (○) Homogeneous EF with CF cathode, Pt anode, [Fe^{2+}] = 0.2 mmol L^{-1}, pH_0 = 3 ; (Δ) Heterogeneous EF with $Fe^{II}Fe^{III}$-LDH modified CF cathode, Pt anode, [Fe^{2+}] = 0 mmol L^{-1}, pH_0 = 7.9 ; (□) Reference experiment with CF cathode, Pt anode, [Fe^{2+}] = 0 mmol L^{-1}, pH_0 = 7.9. Three homogeneous EF experiments were performed in order to assess the reproducibility of the experimental procedure. Standard deviations are reported in Figure 1A.

(B) j = 4.2 mA cm^{-2} : (○) Homogeneous EF with CF cathode, Pt anode, [Fe^{2+}] = 0.2 mmol L^{-1}, pH_0 = 3 ; (Δ) Heterogeneous EF with $Fe^{II}Fe^{III}$-LDH modified CF cathode, Pt anode, [Fe^{2+}]= 0 mmol L^{-1}, pH_0 = 7.9 ; (□) Heterogeneous EF/AO with $Fe^{II}Fe^{III}$-LDH modified CF cathode, Ti_4O_7 anode, [Fe^{2+}] = 0 mmol L^{-1}, pH_0 = 7.9.

One of the main challenges for EAOPs is to reduce the energy consumption (EC). The EC was expressed as kWh per g of DOC removed and calculated from Eq. 6 (Brillas et al., 2009).

296 EC_{DOC} (kWh g^{-1} of DOC) $= \frac{E_{cell}It}{V\Delta(DOC)_{exp}}$ (Eq. 6)

297 where E_{cell} is the average cell voltage (V), I the applied current (A), t the duration of
298 electrolysis (h), V the volume of solution treated (L) and $\Delta(DOC)_{exp}$ the experimental decays
299 of DOC (mgC L^{-1}).

300 For example, 96% removal of DOC by heterogeneous EF at 8.3 mA cm^{-2} required 0.35 kWh
301 g^{-1} of DOC removed. By comparison, 77% DOC removal by heterogeneous EF/AO using
302 Ti_4O_7 anode at 4.2 mA cm^{-2} required only 0.13 kWh g^{-1} of DOC. This value decreased to 0.11
303 kWh g^{-1} of DOC for 45% removal of DOC by the same process (4 h of treatment instead of 8
304 h). In fact, high current density strongly increased energy consumption because of
305 concomitant rise in total cell voltage (from 7.2 to 10.4 V). Parasitic reaction such as hydrogen
306 evolution, 4 e^- reduction of O_2 to H_2O and 2 e^- oxidation of water to O_2 are also promoted at
307 higher current density. Moreover, at high removal rate of DOC and low residual DOC, the
308 current efficiency is strongly decreased by mass transport limitations. Therefore, in order to
309 achieve high DOC removal rate with low energy consumption, it was proposed to combine
310 EAOPs with a biological post-treatment, since EAOPs are able to transform biorefractory
311 organic compounds into by-products that are more biodegradable than initial compounds
312 (Ganzenko et al., 2014; Olvera-Vargas et al., 2015; Trellu et al., 2016a). In practice, that
313 would mean implementing the EAOP as a preliminary treatment before recirculation of the
314 NF concentrate towards the MBR. Thus, the next objective of this study was to monitor the
315 evolution of the biodegradability of the effluent, as well as to better understand the evolution
316 of organic and inorganic compounds during EAOPs.

317

318

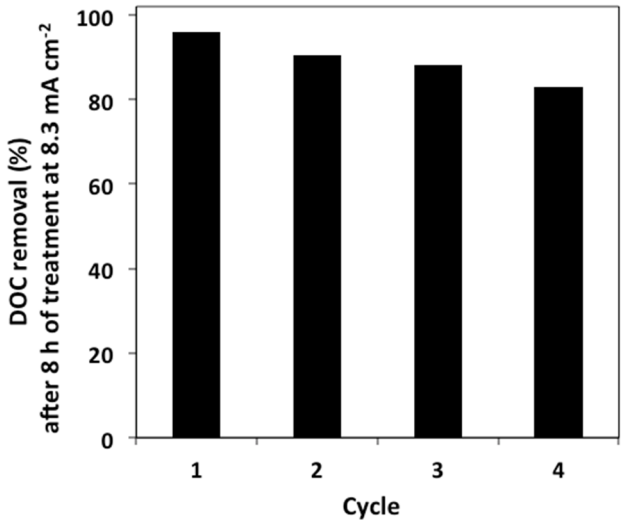

Figure 2 – DOC removal after 8h of electrolysis *vs* number of cycles for the heterogeneous EF treatment using $Fe^{II}Fe^{III}$-LDH/CF cathode and Pt anode at 8.3 mA cm^{-2}.

3.3 Biodegradability enhancement

Respirometric measurements performed have the advantage of being a direct and rapid biological assessment of aerobic degradation under similar conditions than in the real industrial MBR (Reuschenbach et al., 2003). The calculated biodegradability enhancement (BE) values are presented in Fig. 3 after 4 and 8h of treatment for different EAOP configurations and current densities applied.

In all cases, heterogeneous EF shows an increase in the biodegradability of the NF concentrate, which validate the potenital positive role of EAOPs as a pre-treatment before recirculating the NF concentrate to the MBR. In general the more the mineralization rate is achieved the more the biodegradability enhancement is observed. After 8 h of treatment by heterogeneous EF at 4.2 mA cm^{-2}, the BE index reached 11 with Ti_4O_7 anode, compared to 5.9 with Pt anode, which validate the positive effect of combining EF with AO. We could

333 state that a satisfactory biodegradability enhancement (between 4.1 and 9.1) was reached after

334 4 h with optimal energy consumption efficiency.

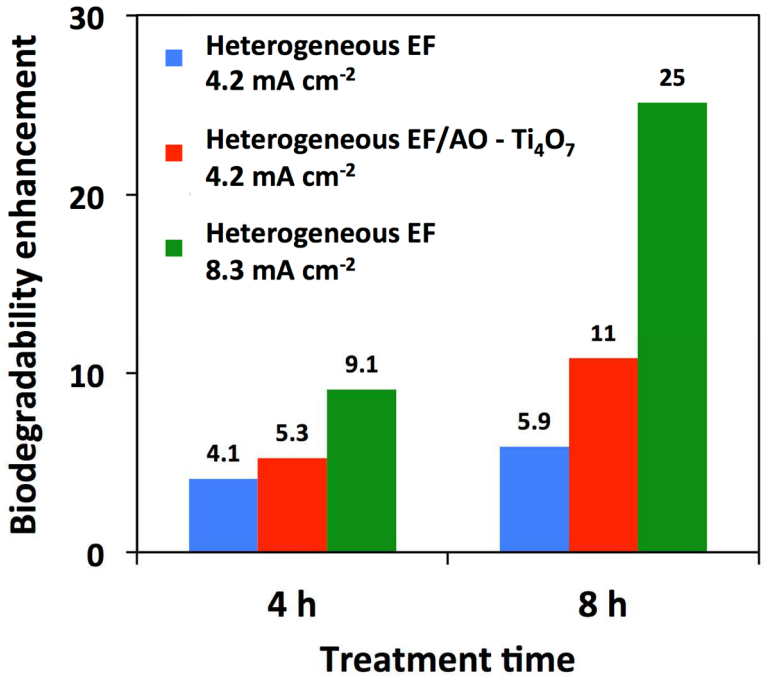

335 **Figure 3** – Biodegradability enhancement at two different treatment times for different

336 EAOPs and current densities.

337

338

339 **3.4 Acute toxicity of the effluent**

340 Toxicity evolution of the NF concentrate during its electrolysis by both heterogeneous and

341 homogeneous EF was evaluated by Microtox® standard method (Fig. 4). Initially (i.e. before

342 any treatment of the NF concentrate), around 50±5% of *V. fischeri* luminescence inhibition

343 was observed because of the presence of large amount of toxic trace metals and organic

344 pollutants. *V. fischeri* luminescence inhibition can be sensitive to various phenomena that can

345 not be controlled and studied separately during the treatment of such complex effluent, e.g.

346 the removal of toxic organic pollutants, the formation of toxic degradation by-products, the

347 formation of non-toxic degradation by-products (which could promote stimulation of bacterial
348 luminescence), the release of inorganic compounds and the evolution of metal speciation.
349 Therefore, it is difficult to draw reliable conclusions from these analyses. However, results
350 show that EAOPs are not able to remove completely the acute toxicity from such complex
351 effluent containing both organic and inorganic toxic compounds. Luminescence inhibtion
352 might even increases significantly, particularly after achieving high mineralization rates (for
353 example during heterogeneous EF at 8.3 mA cm^{-2} and heterogeneous EF at 4.2 mA cm^{-2}).
354 From the comparison of heterogeneous EF experiments performed with either Pt or Ti_4O_7
355 anode, it seems that anodic oxidation participate to avoid the accumulation of toxic by-
356 products in the bulk.

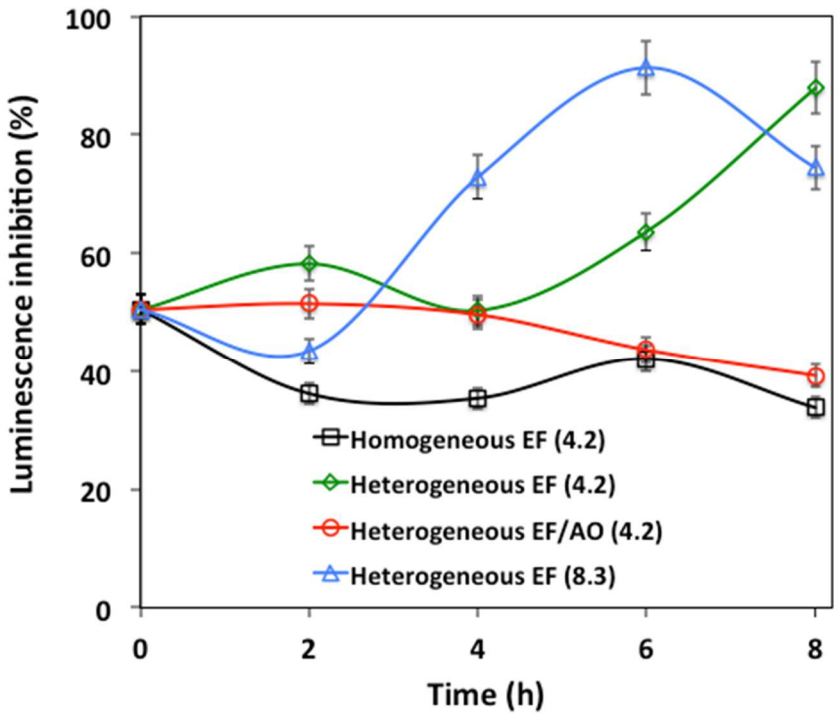

Figure 4 – Evolution of *Vibrio fisheri* luminescence inhibition (Microtox® test) *vs* electrolysis time according to EAOP configuration and current density (in brackets, mA cm^{-2})

357

358

3.5 Characterization of the organic matter by 3DEEM

3DEEM has been reported to be a useful tool for characterization of colloidal and dissolved organic matter. Particularly, Jacquin et al. (2017) recently emphasized a correlation between the volume of fluorescence of zone III' (HA+FA-like fluorophores) and the concentration in a full-scale MBR of humic substances (MW ≈ 1000 Da) and building blocks (degradation by-products from humic substances, with MW ≈ 300-500 Da) measured by size exclusion liquid chromatography coupled with organic carbon and organic nitrogen detector. Similarly, a correlation was also obtained between the volume of fluorescence of zone II' (SMP-like fluorophores) and the concentration of proteins from biopolymers (MW ≈ 20,000 - 7.5 x 10^{11} Da). Besides, no correlation was obtained for the volume of fluorescence of zone I' because fluorophores of this zone would be mostly associated with colloidal proteins that could not be analyzed by size exclusion liquid chromatography (Jacquin et al., 2017). In this study, we proposed to use these results with the view to obtain indications on the evolution of the nature of the organic matter during EAOPs.

The initial effluent was mainly constituted of HA+FA-like fluorophores from zone III' as shown in Fig. 5A and 5B. This result is consistent with the pre-treatment of the effluent in the MBR because microfiltration membranes have lower retention capacity for these low MW compounds. A strong decrease of fluorophores of zone III' was then observed during both heterogeneous EF (Fig. 5C) and EF/AO (Fig. 5D) due to (i) precipitation of humic acids at acidic pH and (ii) fast degradation and mineralization of these low MW compounds with an aromatic structure that reacts quickly with $^{\bullet}OH$ (Trellu et al., 2016b). By comparison, fluorescence from colloidal proteins of zone I' decreased much more slowly. This phenomenon might be ascribed to the lower availability of colloids for reaction with $^{\bullet}OH$ in the aqueous phase. In the context of the global combined process, this result means that improving the retention of colloidal proteins in the MBR would then have a positive effect on

the efficiency of the EAOP. Finally, it was also observed that the use of Ti_4O_7 anode for the heterogeneous AO/EF process promoted significantly the decrease of the fluorescence of proteins from biopolymers (zone II', Fig. 5D). This might be ascribed to the higher electro-catalytic activity of Ti_4O_7 for anodic oxidation of organic compounds, compared to Pt anode (Ganiyu et al., 2016).

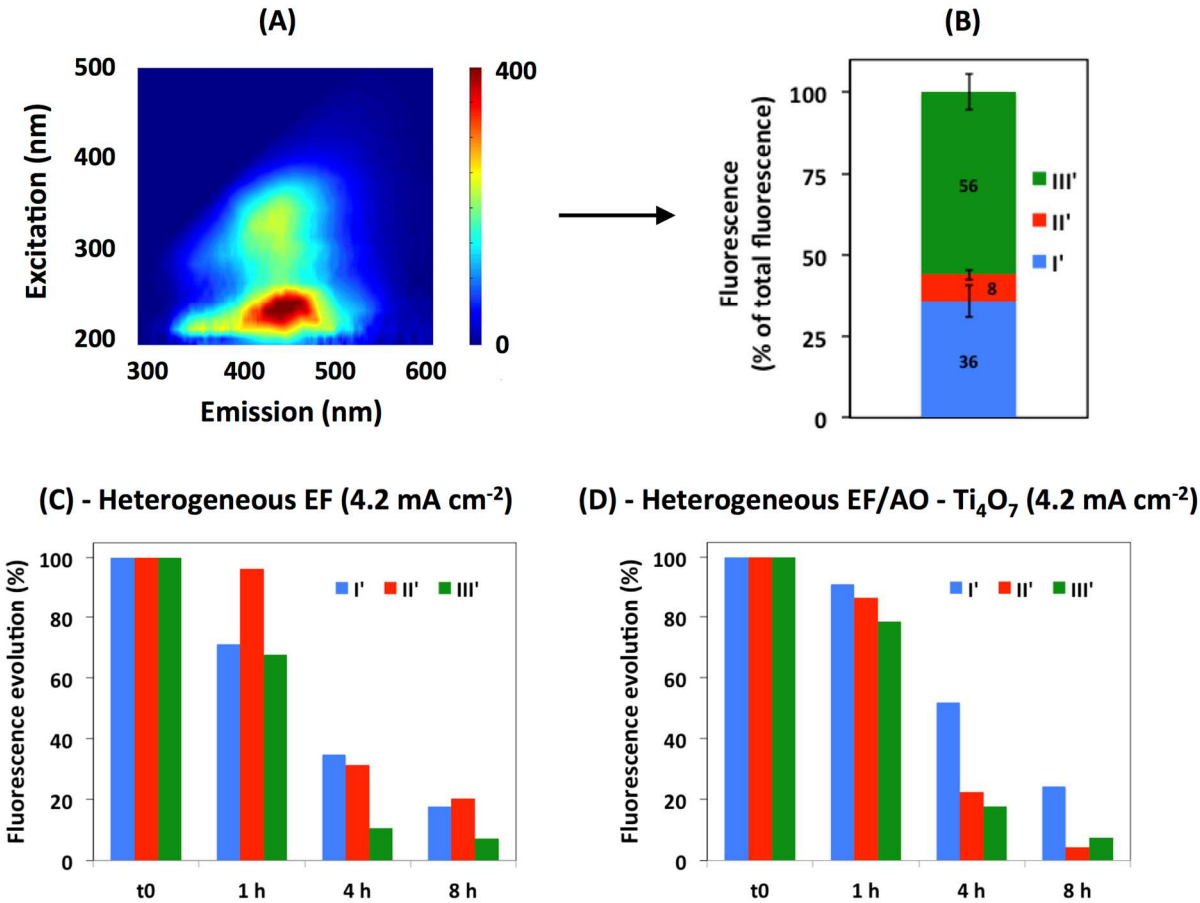

Figure 5 – Fluorescence evolution of the NF concentrate effluent treated by EAOPs, as a function of time treatment. Zone I': colloidal proteins ; zone II': Soluble Microbial by-Product (SMP)-like fluorophores ; zone III': Humic and Fulvic acids (HA + FA)-like fluorophores.

396 **3.6 Identification and quantification of short-chain carboxylic acids**

397 Short-chain carboxylic acids are common degradation by-products generated during the
398 degradation of organic compounds by EAOPs (Oturan et al., 2008). In this study, they were
399 identified by ion-exclusion HPLC and chromatograms revealed five well defined peaks
400 corresponding to acetic, formic, succinic, malonic and oxamic acids. Results were firstly
401 analyzed by following the evolution of the concentration of the sum of carboxylic acids
402 analyzed. The evolution of the concentration according to treatment time was determined for
403 homogeneous EF at 8.3 mA cm^{-2}. An initial increase of the concentration was observed until t
404 = 6 h ([Σ carboxylic acids] = 55 mgC L^{-1}) because of the degradation of aromatic pollutants.
405 Then, the concentration decreased ([Σ carboxylic acids] = 34 mgC L^{-1} at t = 8 h). In fact, the
406 lower concentration of organic compounds after 6 hours of treatment resulted in lower
407 formation rate of carboxylic acids compared to the degradation rate. Interestingly, Fig. 6A
408 shows a linear correlation (R^2 = 0.92) between DOC removal (%) and proportion of
409 carboxylic acids among the residual DOC. This correlation took into consideration all
410 analyzes performed for the different configurations tested. The higher the DOC removal
411 achieved, the higher was the proportion of carboxylic acids among the residual DOC. This
412 result is consistent with the lower reaction rate constant of short-chain carboxylic acids with
413 $^{\bullet}OH$ (10^7 - 10^8 M^{-1} s^{-1}) compared to aromatic compounds (10^9 - 10^{10} M^{-1} s^{-1}) from which they
414 are formed (Oturan et al., 2008). The evolution of the proportion of each single carboxylic
415 acid was also studied (Fig. 6B). It was noticed that the proportion of acetic acid among total
416 carboxylic acid concentration was continuously increased over time during homogeneous EF
417 at 8.3 mA cm^{-2}. This phenomenon is also consistent with the lower reaction rate constant of
418 acetic acid with $^{\bullet}OH$ (1.6 x 10^7 M^{-1} s^{-1}) compared to other carboxylic acids (Oturan et al.,
419 2008). Similar trend was observed after 8 h of electrolysis using heterogeneous EF at 8.3 mA
420 cm^{-2} or 4.2 mA cm^{-2} and homogeneous EF at 4.2 mA cm^{-2}, i.e. the higher the DOC removal

421 rate (Fig. 1), the higher the proportion of acetic acid. Heterogeneous EF/AO using Ti_4O_7 was
422 the only experiment exhibiting a different trend, thus indicating that Ti_4O_7 might modify
423 mineralization mechanisms, compared to Pt anode. Higher proportion of N-containing oxamic
424 acid and lower proportion of acetic acid were observed with Ti_4O_7 anode, which might be
425 attributed to the better electro-catalytic ability of Ti_4O_7 anode for the degradation of organic
426 nitrogen and acetic acid, compared to Pt anode. As regards to oxamic acid, these results were
427 consistent with 3DEEM. In fact, Ti_4O_7 anode further degraded proteins from biopolymers
428 (zone II'), which usually contain high concentration of N (ratio C/N around 3) (Jacquin et al.,
429 2017). Overall, the increase of the proportion of carboxylic acids over time confirms the
430 suitability of the combination of EAOPs with a biological treatment (Fig. 3), because of the
431 well-known high biodegradability of such compounds.

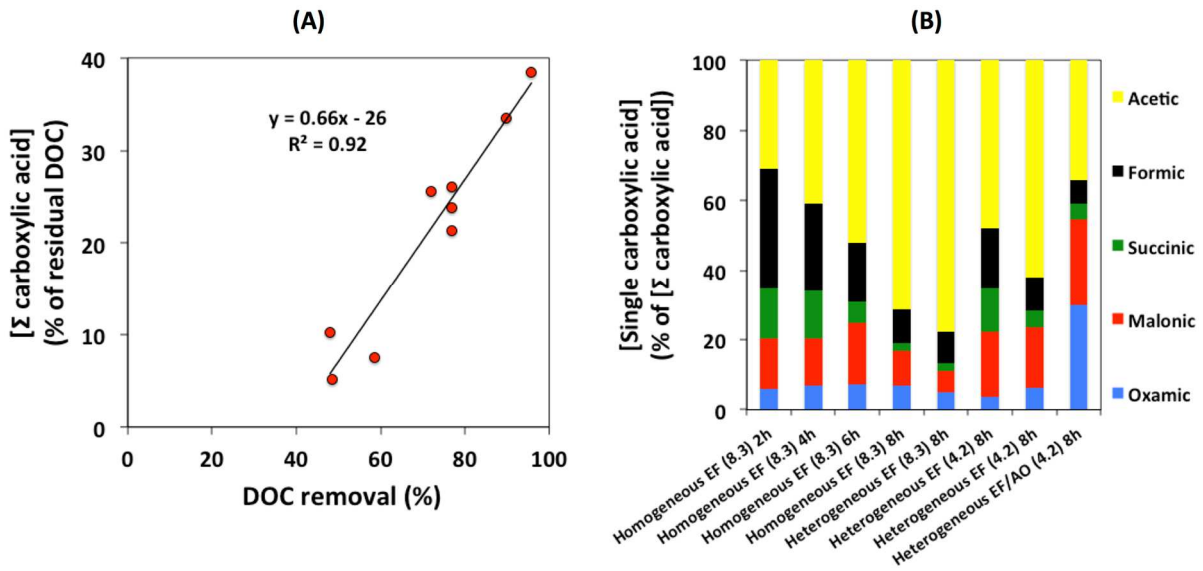

432

433 **Figure 6 –** Generation of short-chain carboxylic acids during EAOPs: (A) correlation
434 between DOC removal (%) and proportion of carboxylic acids among the residual DOC;
435 (B) evolution of the proportion of each single carboxylic acid among the total carboxylic acid
436 concentration as a function of configurations and operating conditions (current density in
437 bracket, mA cm^{-2}).

3.7 Evolution of inorganic species

Mineralization of Cl^- and N-containing organic compounds was accompanied by the formation of inorganic ions. The main inorganic species of interest (NO_3^-, NH_4^+, ClO_3^- and ClO_4^-) were analyzed by ion chromatography. Results are presented in Fig. 7. In all experiments, a stronger increase of the concentration of NH_4^+ was observed compared to NO_3^- (Fig. 7A and 7B). These results can be explained by (i) the direct release of NH_4^+ from mineralization of organic nitrogen and (ii) the release of NO_3^- followed by reduction of NO_3^- into NH_4^+ at the cathode. Actually, the latter reaction is often observed during EF and AO, while oxidation of NH_4^+ at the anode is hindered by the positive charge of this ion (Martin de Vidales et al., 2016; Mousset et al., 2018). The amount of NH_4^+ in the solution increased with treatment time and current density because of the higher mineralization rate of organic nitrogen (Fig. 7B). Higher concentration of NH_4^+ was also obtained using Ti_4O_7 anode (heterogeneous EF/AO), compared to Pt anode (heterogeneous EF). This phenomenon is consistent with the results obtained from 3DEEM and with the higher concentration of oxamic acid previously reported, and supports the higher electro-catalytic activity of Ti_4O_7 for the degradation of organic nitrogen. In the context of a treatment strategy including a recirculation of the effluent back to the MBR, the release of NH_4^+ during EAOPs would require further biological nitrification in the MBR.

Oxidation of Cl^- resulted in a strong increase of ClO_3^- concentration (Fig. 7C). The reaction mechanisms usually go through Cl^- oxidation into Cl_2, followed by hydrolysis of Cl_2 into hypochlorous acid HOCl. Further oxidation of HOCl lead to the formation of ClO_2^- (which was not detected because of the fast oxidation kinetic) and subsequently ClO_3^-. No formation of ClO_4^- was detected in any experiment because higher current density (> 30 mA cm^{-2}) is required to form this compound (Mousset et al., 2018). Besides, it was also observed that the formation of ClO_3^- mainly occurred between 4 and 8 h of treatment, most probably because of

463 the preferential reaction of HOCl with organic species and NH_4^+ (break-point chlorination)
464 between 4 and 8 h of treatment (Martin de Vidales et al., 2016; Mousset et al., 2018). These
465 results confirm the suitability to stop the treatment after 4 h of treatment in order to avoid the
466 accumulation of ClO_3^- and NH_4^+. While ClO_3^- can be toxic for the biomass in the MBR, the
467 formation of NH_3 at basic pH is also highly toxic for the autotrophic biomass (Jacquin et al.,
468 2018).

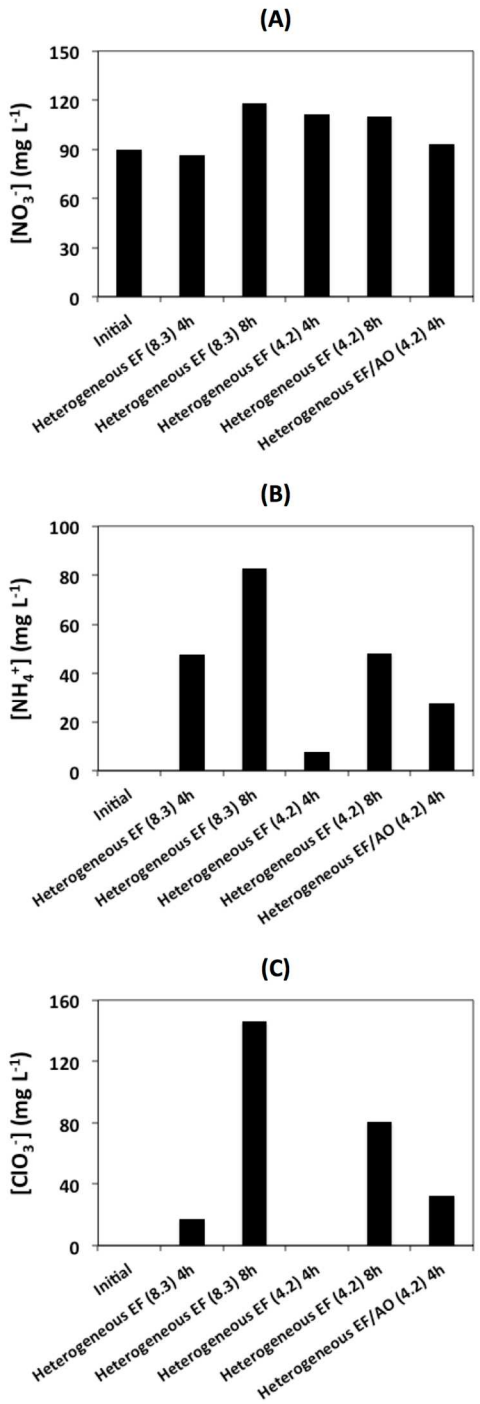

469 **Figure 7** – Concentration evolution of main inorganic species of interest during EAOPs as a
470 function of configurations and operating conditions (current density in bracket, mA cm^{-2}): (A)
471 ClO_3^-, (B) NO_3^- and (C) NH_4^+. ClO_4^- was not detected.

472

473

4. Conclusion

NF concentrate of landfill leachate pre-treated in a MBR contains high concentration of biorefractory organic pollutants that makes very difficult to treat or detoxify by conventional techniques. The investigation of different configurations of EAOPs applied to this complex effluent showed that heterogeneous EF/AO using Ti_4O_7 anode and $Fe^{II}Fe^{III}$-LDH modified CF cathode is the most efficient process for mineralization of organic pollutants. Without initial pH adjustment and external addition of Fe^{2+} in the bulk, 45% removal of DOC was achieved at 4.2 mA cm^{-2} with limited energy consumption (0.11 kWh g^{-1} of DOC removed, i.e. 49.5 kWh m^{-3}). Up to 96% removal of DOC was also obtained by using higher current density (8.3 mA cm^{-2}) during the heterogeneous EF process. The use of Ti_4O_7 anode appeared to be a key parameter for improving the degradation and mineralization of organic nitrogen. From 3DEEM analysis, colloidal proteins were observed to be the most refractory organic compounds. Therefore, improving the retention of such compounds in the MBR could improve the efficiency of the EAOP.

The acute toxicity of the effluent was not removed but strong biodegradability enhancement was observed after 4 h of treatment by heterogeneous EF/AO, thus making possible the recirculation of the residual DOC towards the MBR in order to achieve total COD removal without longer electrochemical treatment time. This result was consistent with the identification and quantification of more biodegradable and less toxic by-products such as carboxylic acids. In fact, a linear correlation was observed between DOC removal rate and proportion of carboxylic acids in the residual DOC. As regards to the fate of inorganic species, the formation of ClO_3^- could be limited by stopping electro-oxidation at 4 h, but enhanced nitrification would be required in the MBR because of the release of NH_4^+ from mineralization of organic nitrogen. Overall, these results emphasized the interdependence

between the MBR process and the EAOP in a combined treatment strategy and demonstrated that the use of EAOPs using suitable electrode materials can be useful for the management of such complex effluent.

Acknowledgements

We gratefully acknowledge the National French Agency of Research 'ANR' for funding the project ECOTS/CELECTRON. Authors are also grateful to Saint Gobain Research Provence for supplying Ti_4O_7 electrodes.

References

Amaral, M.C., Moravia, W.G., Lange, L.C., Zico, M.R., Magalhães, N.C., Ricci, B.C., Reis, B.G., 2016. Pilot aerobic membrane bioreactor and nanofiltration for municipal landfill leachate treatment. Journal of Environmental Science and Health, Part A 51, 640–649.

Ammar, S., Oturan, M.A., Labiadh, L., Guersalli, A., Abdelhedi, R., Oturan, N., Brillas, E., 2015. Degradation of tyrosol by a novel electro-Fenton process using pyrite as heterogeneous source of iron catalyst. Water Research 74, 77–87. https://doi.org/10.1016/j.watres.2015.02.006

Brillas, E., Sirés, I., Oturan, M.A., 2009. Electro-Fenton Process and Related Electrochemical Technologies Based on Fenton's Reaction Chemistry. Chemical Reviews 109, 6570–6631. https://doi.org/10.1021/cr900136g

Campagna, M., Çakmakcı, M., Büşra Yaman, F., Özkaya, B., 2013. Molecular weight distribution of a full-scale landfill leachate treatment by membrane bioreactor and nanofiltration membrane. Waste Management 33, 866–870. https://doi.org/10.1016/j.wasman.2012.12.010

Chen, W., Westerhoff, P., Leenheer, J.A., Booksh, K., 2003. Fluorescence Excitation−Emission Matrix Regional Integration to Quantify Spectra for Dissolved Organic Matter. Environmental Science & Technology 37, 5701–5710. https://doi.org/10.1021/es034354c

Comninellis, C., Kapalka, A., Malato, S., Parsons, S.A., Poulios, I., Mantzavinos, D., 2008. Advanced oxidation processes for water treatment: Advances and trends for R&D. J. Chem. Technol. Biotechnol. 83, 769–776. https://doi.org/10.1002/jctb.1873

Cui, Y.-H., Xue, W.-J., Yang, S.-Q., Tu, J.-L., Guo, X.-L., Liu, Z.-Q., 2018. Electrochemical/peroxydisulfate/Fe3+ treatment of landfill leachate nanofiltration concentrate after ultrafiltration. Chemical Engineering Journal 353, 208–217. https://doi.org/10.1016/j.cej.2018.07.101

Ganiyu, S.O., Huong Le, T.X., Bechelany, M., Oturan, N., Papirio, S., Esposito, G., van Hullebusch, E., Cretin, M., Oturan, M.A., 2018. Electrochemical mineralization of sulfamethoxazole over wide pH range using FeIIFeIII LDH modified carbon felt cathode: Degradation pathway, toxicity and reusability of the modified cathode. Chemical Engineering Journal 350, 844–855. https://doi.org/10.1016/j.cej.2018.04.141

Ganiyu, S.O., Le, T.X.H., Bechelany, M., Esposito, G., Hullebusch, E.D. van, Oturan, M.A., Cretin, M., 2017a. A hierarchical CoFe-layered double hydroxide modified carbon-felt cathode for heterogeneous electro-Fenton process. J. Mater. Chem. A 5, 3655–3666. https://doi.org/10.1039/C6TA09100H

Ganiyu, S.O., Oturan, N., Raffy, S., Cretin, M., Esmilaire, R., van Hullebusch, E., Esposito, G., Oturan, M.A., 2016. Sub-stoichiometric titanium oxide (Ti4O7) as a suitable ceramic anode for electrooxidation of organic pollutants: A case study of kinetics, mineralization and

toxicity assessment of amoxicillin. Water Research 106, 171–182. https://doi.org/10.1016/j.watres.2016.09.056

Ganiyu, S.O., Oturan, N., Raffy, S., Esposito, G., van Hullebusch, E.D., Cretin, M., Oturan, M.A., 2017b. Use of Sub-stoichiometric Titanium Oxide as a Ceramic Electrode in Anodic Oxidation and Electro-Fenton Degradation of the Beta-blocker Propranolol: Degradation Kinetics and Mineralization Pathway. Electrochimica Acta 242, 344–354. https://doi.org/10.1016/j.electacta.2017.05.047

Ganiyu, S. O., Zhou, M., Martínez-Huitle, C. A., 2018. Heterogeneous electro-Fenton and photoelectro-Fenton processes: a critical review of fundamental principles and application for water/wastewater treatment. Applied Catalysis B: Environmental 235, 103-129. https://doi.org/10.1016/j.apcatb.2018.04.044

Ganzenko, O., Huguenot, D., van Hullebusch, E.D., Esposito, G., Oturan, M.A., 2014. Electrochemical advanced oxidation and biological processes for wastewater treatment: a review of the combined approaches. Environmental Science and Pollution Research 21, 8493–8524. https://doi.org/10.1007/s11356-014-2770-6

Ganzenko, O., Trellu, C., Papirio, S., Oturan, N., Huguenot, D., van Hullebusch, E.D., Esposito, G., Oturan, M.A., 2018. Bioelectro-Fenton: evaluation of a combined biological—advanced oxidation treatment for pharmaceutical wastewater. Environmental Science and Pollution Research 25, 20283–20292. https://doi.org/10.1007/s11356-017-8450-6

García-Rodríguez, O., Bañuelos, J.A., El-Ghenymy, A., Godínez, L.A., Brillas, E., Rodríguez-Valadez, F.J., 2016. Use of a carbon felt–iron oxide air-diffusion cathode for the mineralization of Malachite Green dye by heterogeneous electro-Fenton and UVA photoelectro-Fenton processes. Journal of Electroanalytical Chemistry 767, 40–48. https://doi.org/10.1016/j.jelechem.2016.01.035

Guo, L., Jing, Y., Chaplin, B.P., 2016. Development and Characterization of Ultrafiltration TiO2 Magnéli Phase Reactive Electrochemical Membranes. Environ. Sci. Technol. 50, 1428–1436. https://doi.org/10.1021/acs.est.5b04366

Hu, Y., Lu, Y., Liu, G., Luo, H., Zhang, R., Cai, X., 2018. Effect of the structure of stacked electro-Fenton reactor on treating nanofiltration concentrate of landfill leachate. Chemosphere 202, 191–197. https://doi.org/10.1016/j.chemosphere.2018.03.103

Iglesias, O., Fernández de Dios, M.A., Pazos, M., Sanromán, M.A., 2013. Using iron-loaded sepiolite obtained by adsorption as a catalyst in the electro-Fenton oxidation of Reactive Black 5. Environmental Science and Pollution Research 20, 5983–5993. https://doi.org/10.1007/s11356-013-1610-4

Jacquin, C., Lesage, G., Traber, J., Pronk, W., Heran, M., 2017. Three-dimensional excitation and emission matrix fluorescence (3DEEM) for quick and pseudo-quantitative determination of protein- and humic-like substances in full-scale membrane bioreactor (MBR). Water Research 118, 82–92. https://doi.org/10.1016/j.watres.2017.04.009

Jacquin, C., Monnot, M., Hamza, R., Kouadio, Y., Zaviska, F., Merle, T., Lesage, G., Héran, M.,

2018. Link between dissolved organic matter transformation and process performance in a membrane bioreactor for urinary nitrogen stabilization. Environmental Science: Water Research & Technology 4, 806–819. https://doi.org/10.1039/C8EW00029H

Kjeldsen, P., Barlaz, M.A., Rooker, A.P., Baun, A., Ledin, A., Christensen, T.H., 2002. Present and Long-Term Composition of MSW Landfill Leachate: A Review. Critical Reviews in Environmental Science and Technology 32, 297–336. https://doi.org/10.1080/10643380290813462

Li, X., Zhu, W., Wu, Y., Wang, C., Zheng, J., Xu, K., Li, J., 2015. Recovery of potassium from landfill leachate concentrates using a combination of cation-exchange membrane electrolysis and magnesium potassium phosphate crystallization. Separation and Purification Technology 144, 1–7. https://doi.org/10.1016/j.seppur.2015.01.035

Ma, L., Zhou, M., Ren, G., Yang, W., Liang, L., 2016. A highly energy-efficient flow-through electro-Fenton process for organic pollutants degradation. Electrochimica Acta 200, 222–230. https://doi.org/10.1016/j.electacta.2016.03.181

Mahindrakar, K.V., Rathod, V.K., 2018. Utilization of banana peels for removal of strontium (II) from water. Environmental Technology & Innovation 11, 371–383. https://doi.org/10.1016/j.eti.2018.06.015

Martin de Vidales, M.J., Millán, M., Sáez, C., Cañizares, P., Rodrigo, M.A., 2016. What happens to inorganic nitrogen species during conductive diamond electrochemical oxidation of real wastewater? Electrochemistry Communications 67, 65–68. https://doi.org/10.1016/j.elecom.2016.03.014

Martínez-Huitle, C.A., Rodrigo, M.A., Sirés, I., Scialdone, O., 2015. Single and Coupled Electrochemical Processes and Reactors for the Abatement of Organic Water Pollutants: A Critical Review. Chem. Rev. 115, 13362–13407. https://doi.org/10.1021/acs.chemrev.5b00361

Mousset, E., Pontvianne, S., Pons, M.-N., 2018. Fate of inorganic nitrogen species under homogeneous Fenton combined with electro-oxidation/reduction treatments in synthetic solutions and reclaimed municipal wastewater. Chemosphere 201, 6–12. https://doi.org/10.1016/j.chemosphere.2018.02.142

Oller, I., Malato, S., Sánchez-Pérez, J.A., 2011. Combination of Advanced Oxidation Processes and biological treatments for wastewater decontamination—A review. Science of The Total Environment 409, 4141–4166. https://doi.org/10.1016/j.scitotenv.2010.08.061

Olvera-Vargas, H., Cocerva, T., Oturan, N., Buisson, D., Oturan, M.A., 2015. Bioelectro-Fenton: A sustainable integrated process for removal of organic pollutants from water: Application to mineralization of metoprolol. J. Hazard. Mater. https://doi.org/10.1016/j.jhazmat.2015.12.010

Oturan, M.A., Pimentel, M., Oturan, N., Sirés, I., 2008. Reaction sequence for the mineralization of the short-chain carboxylic acids usually formed upon cleavage of aromatics during electrochemical Fenton treatment. Electrochimica Acta 54, 173–182.

https://doi.org/10.1016/j.electacta.2008.08.012

Oturan, N., van Hullebusch, E.D., Zhang, H., Mazeas, L., Budzinski, H., Le Menach, K., Oturan, M.A., 2015. Occurrence and Removal of Organic Micropollutants in Landfill Leachates Treated by Electrochemical Advanced Oxidation Processes. Environmental Science & Technology 49, 12187–12196. https://doi.org/10.1021/acs.est.5b02809

Özcan, A., Sahin, Y., Koparal, A.S., Oturan, M.A., 2008. Propham mineralization in aqueous medium by anodic oxidation using boron-doped diamond anode: Influence of experimental parameters on degradation kinetics and mineralization efficiency. Water Res. 42, 2889–2898. https://doi.org/10.1016/j.watres.2008.02.027

Panizza, M., Cerisola, G., 2009. Direct and mediated anodic oxidation of organic pollutants. Chem. Rev. 109, 6541–6569. https://doi.org/10.1021/cr9001319

Ponthieu, M., Pinel-Raffaitin, P., Le Hecho, I., Mazeas, L., Amouroux, D., Donard, O.F.X., Potin-Gautier, M., 2007. Speciation analysis of arsenic in landfill leachate. Water Research 41, 3177–3185. https://doi.org/10.1016/j.watres.2007.04.026

Poza-Nogueiras, V., Rosales, E., Pazos, M., Sanromán, M. Á. (2018). Current advances and trends in electro-Fenton process using heterogeneous catalysts–a review. Chemosphere 201, 399-416. https://doi.org/10.1016/j.chemosphere.2018.03.002

Radjenovic, J., Sedlak, D.L., 2015. Challenges and Opportunities for Electrochemical Processes as Next-Generation Technologies for the Treatment of Contaminated Water. Environ. Sci. Technol. 49, 11292–11302. https://doi.org/10.1021/acs.est.5b02414

Reuschenbach, P., Pagga, U., Strotmann, U., 2003. A critical comparison of respirometric biodegradation tests based on OECD 301 and related test methods. Water Research 37, 1571–1582. https://doi.org/10.1016/S0043-1354(02)00528-6

Sirés, I., Brillas, E., Oturan, M.A., Rodrigo, M.A., Panizza, M., 2014. Electrochemical advanced oxidation processes: today and tomorrow. A review. Environ Sci Pollut Res 21, 8336–8367. https://doi.org/10.1007/s11356-014-2783-1

Trellu, C., Chaplin, B.P., Coetsier, C., Esmilaire, R., Cerneaux, S., Causserand, C., Cretin, M., 2018a. Electro-oxidation of organic pollutants by reactive electrochemical membranes. Chemosphere 208, 159–175. https://doi.org/10.1016/j.chemosphere.2018.05.026

Trellu, C., Coetsier, C., Rouch, J.-C., Esmilaire, R., Rivallin, M., Cretin, M., Causserand, C., 2018b. Mineralization of organic pollutants by anodic oxidation using reactive electrochemical membrane synthesized from carbothermal reduction of TiO2. Water Research 131, 310–319. https://doi.org/10.1016/j.watres.2017.12.070

Trellu, C., Ganzenko, O., Papirio, S., Pechaud, Y., Oturan, N., Huguenot, D., van Hullebusch, E.D., Esposito, G., Oturan, M.A., 2016a. Combination of anodic oxidation and biological treatment for the removal of phenanthrene and Tween 80 from soil washing solution. Chemical Engineering Journal 306, 588–596. https://doi.org/10.1016/j.cej.2016.07.108

Trellu, C., Oturan, N., Pechaud, Y., van Hullebusch, E.D., Esposito, G., Oturan, M.A., 2017.

Anodic oxidation of surfactants and organic compounds entrapped in micelles – Selective degradation mechanisms and soil washing solution reuse. Water Research 118, 1–11. https://doi.org/10.1016/j.watres.2017.04.013

Trellu, C., Péchaud, Y., Oturan, N., Mousset, E., Huguenot, D., van Hullebusch, E.D., Esposito, G., Oturan, M.A., 2016b. Comparative study on the removal of humic acids from drinking water by anodic oxidation and electro-Fenton processes: Mineralization efficiency and modelling. Applied Catalysis B: Environmental 194, 32–41. https://doi.org/10.1016/j.apcatb.2016.04.039

Van der Bruggen, B., Koninckx, A., Vandecasteele, C., 2004. Separation of monovalent and divalent ions from aqueous solution by electrodialysis and nanofiltration. Water Research 38, 1347–1353. https://doi.org/10.1016/j.watres.2003.11.008

Van der Bruggen, B., Lejon, L., Vandecasteele, C., 2003. Reuse, Treatment, and Discharge of the Concentrate of Pressure-Driven Membrane Processes. Environmental Science & Technology 37, 3733–3738. https://doi.org/10.1021/es0201754

Wang, Yujing, Zhao, G., Chai, S., Zhao, H., Wang, Yanbin, 2013. Three-Dimensional Homogeneous Ferrite-Carbon Aerogel: One Pot Fabrication and Enhanced Electro-Fenton Reactivity. ACS Applied Materials & Interfaces 5, 842–852. https://doi.org/10.1021/am302437a

Westerhoff, P., Prapaipong, P., Shock, E., Hillaireau, A., 2008. Antimony leaching from polyethylene terephthalate (PET) plastic used for bottled drinking water. Water Research 42, 551–556. https://doi.org/10.1016/j.watres.2007.07.048

Xu, Y., Chen, C., Li, X., Lin, J., Liao, Y., Jin, Z., 2017. Recovery of humic substances from leachate nanofiltration concentrate by a two-stage process of tight ultrafiltration membrane. Journal of Cleaner Production 161, 84–94. https://doi.org/10.1016/j.jclepro.2017.05.095

Zhang, G., Wang, S., Yang, F., 2012. Efficient Adsorption and Combined Heterogeneous/Homogeneous Fenton Oxidation of Amaranth Using Supported Nano-FeOOH As Cathodic Catalysts. The Journal of Physical Chemistry C 116, 3623–3634. https://doi.org/10.1021/jp210167b

Zhang, H., Fei, C., Zhang, D., Tang, F., 2007. Degradation of 4-nitrophenol in aqueous medium by electro-Fenton method. Journal of Hazardous Materials 145, 227–232. https://doi.org/10.1016/j.jhazmat.2006.11.016

Zhang, L., Li, A., Lu, Y., Yan, L., Zhong, S., Deng, C., 2009. Characterization and removal of dissolved organic matter (DOM) from landfill leachate rejected by nanofiltration. Waste Management 29, 1035–1040. https://doi.org/10.1016/j.wasman.2008.08.020

Zhang, Q.-Q., Tian, B.-H., Zhang, X., Ghulam, A., Fang, C.-R., He, R., 2013. Investigation on characteristics of leachate and concentrated leachate in three landfill leachate treatment plants. Waste Management 33, 2277–2286. https://doi.org/10.1016/j.wasman.2013.07.021